Electrochimica Acta 176 (2015) 727–734

Contents lists available at ScienceDirect

Electrochimica Acta

journal homepage: www.elsevier.com/locate/electacta

Electrospun Nanofibers for Sandwiched Polyimide/Poly (vinylidene fluoride)/Polyimide Separators with the Thermal Shutdown Function

Dezhi Wu[a,b,1], Chuan Shi[c,1], Shaohua Huang[a], Xiaochun Qiu[a], Huan Wang[a], Zhan Zhan[a], Peng Zhang[d], Jinbao Zhao[c], Daoheng Sun[a], Liwei Lin[a,e,*]

[a] School of Physics and Mechanical & Electrical Engineering, Xiamen University, Xiamen 361005, PR China
[b] Shenzhen Research Institute of Xiamen University, Shenzhen 518057, PR China
[c] College of Chemistry & Chemical Engineering, Xiamen University, Xiamen 361005, PR China
[d] School of Energy Research, Xiamen University, Xiamen 361005, PR China
[e] Department of Mechanical Engineering, Berkeley Sensor & Actuator Center, University of California, Berkeley, California 94720, USA

ARTICLE INFO

Article history:
Received 30 January 2015
Received in revised form 13 July 2015
Accepted 13 July 2015
Available online 18 July 2015

Keywords:
Lithium Ion Battery
Separator
Electrospinning
Thermal Shutdown
Nanofiber

ABSTRACT

Nanofibers fabricated by the electrospinning process have been used to construct sandwich-type Polyimide/Poly (vinylidene fluoride)/Polyimide (PI/PVDF/PI) separators with the thermal shutdown function for lithium ion batteries. This architecture uses the good thermal stability of PI as the top and bottom structure layers. Under high temperature operations, the middle layer made of PVDF nanofibers can melt and form a pore-free film to shut down the battery operation. The electrolyte uptake and ionic conductivity of the PI/PVDF/PI separator are superior to those of commercial polyolefin separators at 476% and 3.46 mS cm^{-1}, respectively, resulting better battery performances in terms of impedance, discharge capacity and cycle life. Under high temperature treatments above 170 °C, the self-shutdown function of the PI/PVDF/PI has been observed within 10 minutes, which could serve as the safety mechanism to defend the thermal runaway issue of lithium ion batteries. The effects of heating temperature and different time on the morphologies of each layer and electrolyte uptake of the separator are characterized as well.

Published by Elsevier Ltd.

1. Introduction

Lithium ion batteries (LIBs) have good properties in high energy density, long cycle life and low capacity loss [1] for energy conversion/storage applications in cellular phones, computers, camcorders, and electric vehicles (EVs) [2]. However, the thermal stability of LIBs has been a safety issue, including the incident of battery fires in Boeing 787 plane. Previously, various approaches have been developed to improve the safe operation of LIBs, including electrolyte additives [3], room temperature ionic liquids [4], composite electrodes [5] and new separator designs [6,7]. Among these methods, modification of separators is straightforward and non-chemical with minimum possible degradations to the original battery operations as compared with other chemical approaches. Specifically, separators are responsible for the transfer of lithium ions between the cathode- and anode-electrodes while prevent the physical contacts of the two electrodes to avoid electrical short circuit. Porous polyolefin materials, including polyethylene (PE), polypropylene (PP) and PP/PE/PP composites have been demonstrated and widely applied as separators in LIBs due to its advantages of superb chemical properties, excellent mechanical strength and low cost etc. At the same time, their non-polar and hydrophobic properties and wet/dry fabrication method also bring many critical drawbacks, such as poor thermal stability (operating temperature T_o<110 °C, shutdown temperature for PE T_1<140 °C), low porosity about 40-50% and poor affinity with liquid electrolyte (contact angle θ≈30 °) [8,9]. Their large thermal shrinkage in harsh environment with high temperature will cause direct contact of the electrodes and then thermal runaway happens, which may lead to disaster of fire or explosion. Therefore a separator with shutdown function under high temperature is needed to as a fail-safe tool. On the other hand, their low porosity and hydrophobicity to electrolyte will induce lower electrolyte uptake, thus slower transport for lithium ion will be suffered to makes electrochemical performance worse. Till now, a method to fabricate a separator with high-temperature shutdown function, high porosity and excellent affinity with electrolyte as well is still a challenge.

* Corresponding author. Tel.: +86 5922185927; fax: +86 5922185927.
E-mail address: lwlin@berkeley.edu (L. Lin).
[1] Both authors contribute equally to this work.

http://dx.doi.org/10.1016/j.electacta.2015.07.072
0013-4686/Published by Elsevier Ltd.

Nomenclature

P	porosity of membrane
M_m	the mass of dry membrane, g
M_{BuOH}	mass of absorbed n-butanol, g
ρ_{BuOH}	density of n-butanol, g cm^{-3}
ρ_P	density of polymer, g cm^{-3}
EU	electrolyte uptake of membrane
W_0	mass of dry membrane, g
W	mass of wet electrolyte-absorbed membrane, g
σ	ionic conductivity of separator, S cm^{-1}
L	thickness of separator, cm
R_b	bulk resistance of separator, Ω
S	the area of copper electrode, cm^2

Electrospinning is a cost-effective and versatile process to construct polymer nanofibers as membranes with high porosity [10,11]. Various electrospun membranes from different polymer materials have been attempted as separators to successfully achieve low thermal shrinkage and improved electrolyte uptake, including thermoplastic polyurethane (TPU) [12], polyacrylonitrile (PAN) [13], Poly(vinylidene fluoride) (PVDF) [14], poly(vinylidene fluoride co-hexafluoropropylene) (PVDF-HFP) [15], polyethylene terephthalate (PET) [16] and polyimide (PI) [17]. Trilayer separators basing on electrospun nanofiber membranes have been also explored to further improve the thermal shrinkage and electrochemical performance [18–20]. (PVDF-HFP)/poly (vinyl chloride) (PVC)/(PVDF-HFP) based membranes have been utilized to enhance the mechanical strength and decrease the thermal shrinkage, where PVC with higher melting point helps to improve mechanical integrity [18]. Lee et al. demonstrated an Al_2O_3-nanoparticle-coated polyimide (Al_2O_3-PI) nonwoven membrane with a dip-coating process to gain lower impedance and longer cycle life [19]. To our best knowledge, no literature relating to shutdown behaviour and morphologies changes under different heating temperatures and time has been reported. In this work, electrospun PI nanofibers with high melting temperature and low shrinkage [17] are chosen as the structural supports and a layer of electrospun PVDF with lower melting point than PI is placed in between for the self-shutdown function under high temperature operations, such as thermal runaway. The PVDF layer can melt and

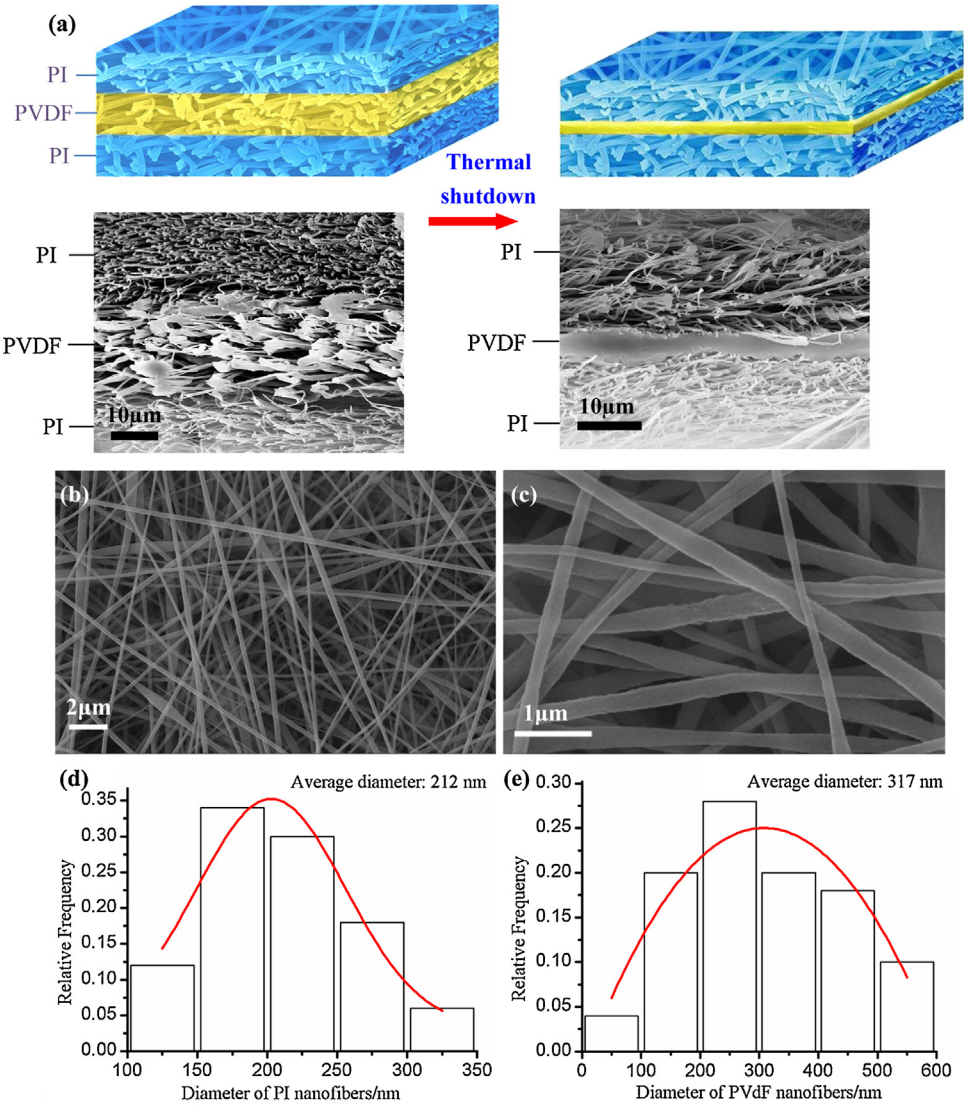

Fig. 1. (a) Illustrations and cross sectional SEM images of the PI/PVDF/PI separator before and after the high temperature melt and shutdown behavior of the PVDF nanofibers layer. (b) & (c) Top view SEM photos of electrospun PI and PVDF nanofibers and (d) & (e) histograms of nanofiber diameter distributions, respectively.

forms an insulated film to seal the pores and block the transfer of ions under high temperature. As a result, the sandwiched PI/PVDF/PI composite membrane can provide both good thermal stability from the structural PI layers and self-shutdown function by the melting of PVDF fibers. The porosity, thermal shrinkage, electrolyte uptake, morphology changes, shutdown electrochemical behaviour, impedance, cycling performance and rate capacity etc. are discussed in details.

2. Experimental

2.1. Preparation of fibrous membranes

PI and dimethylacetamide (DMAc) mixture was purchased from Hangzhou surmount science & technology (Hangzhou, China). PVDF (Mw=500,000, Sensure, Shanghai, China) was dissolved in the mixture of dimethylformamide (DMF) and acetone with a volume ratio of 1:1 to have the final PVDF concentration of 16%, and sealed at room temperature for more than 48 hours with intensive mixing. Sandwiched PI/PVDF/PI composite porous membrane was fabricated by the electrospinning process using PI, PVDF and PI solution separately in sequence. The setup included a pump (Harvard, U.S.A.), a syringe, a high voltage source (Gamma, U.S.A.) and a copper collector which was placed on top of an X-Y motion stage (Googoltech, Shenzhen, China). The anode of the high voltage source was connected to the conductive spinneret and the ground collector was connected to the cathode. The flow rates of the PI solution and PVDF solution were 100 μl h^{-1} and 125 μl h^{-1}, respectively, and the electrospinning processes were conducted under an applied bias of 10 kV with 10 cm of spinneret-to-collector distance. The collector moved back and forth at a speed of 40 cm min^{-1} in the X-axial direction with a moving displacement of 12 cm and moved intermittently in the Y-axial direction (40 μm when the collector reached one end of the X-directional scanning range) for better distribution and uniformity of nanofibers.

2.2. Characterizations

The morphology of the PI/PVDF/PI membrane was observed in LEO 1530 (FE-SEM, Germany). The cross sectional view of the sample was prepared by immersing the membranes in deionized water and refrigerated at -18 °C for 12 hours. Afterwards, the membranes were cut by a sharp and heated at 60 °C for 2 h in a furnace (DHG-9011A, Shanghai Jinghong Instrument, China). The tests on the ionic conductivity of the separator, over the temperature ranging from 30 to 70 °C, have been measured using a sandwiched copper/separator/copper structure in an electrochemical workstation (Metrohm, Switzerland) over the frequency range from 1 to 10^5 Hz with 5 mV of AC inputs. The thermal properties of the original separator were evaluated by differential scanning calorimetry (DSC) and thermal gravimetric analysis (TGA) from ambient temperature to 800 °C at a heating rate of 10 °C min^{-1} in argon atmosphere using SDT Q600 (U.S.A.). The tensile strength was tested by UTM 4000 universal test machine (Sansi Zongheng, China). The solutions of PVDF and PI were used respectively to fabricate compact thin films by following process of being spincoated with three consecutive rotating speeds (500 r/min, 700 r/min and 380 r/min for 10 s, 30 s and 10 s respectively) on spincoater (SC-1B, Beijing), dried completely in atmosphere and soaked in electrolyte for more than two hours. Then the swelling of PI and PVDF can be calculated by the mass changes from the dried film to the said soaked film.

To investigate the electrochemical properties and shutdown behaviors of the battery, CR2016 coin cells were adopted and assembled in a glove box using electrolyte LB-303 purchased from Zhangjiagang Guotai-Huarong New Chemical Materials Co. (Jiangsu, China). The positive electrodes (90 wt.% of $LiMnO_2$, 4 wt.% of acetylene black, 1 wt.% of graphite and 5 wt.% of PVDF) were made on aluminum foils and the counter electrode was lithium metal. Battery cycle performances (0.5C rate) and rate capability were measured by a multi-channel battery cycler (LAND, Wuhan, China).

3. Results and discussion

3.1. Morphology, porosity, electrolyte uptake, swelling and ionic conductivity

Fig. 1a illustrates the PI/PVDF/PI separator before and after the thermal shutdown with the schematic diagrams at the top and SEM cross-sectional view images at the bottom. Initially, the separator has a 20 μm-thick layer made of PVDF nanofibers at the center and two 15 μm-thick layers made of PI nanofibers at the top and bottom. After the thermal treatment process at 170 °C, the PVDF nanofibers are melted to form a pore-free thin film and its thickness is shrunk to about 3.8 μm. The top view SEM images of the electrospun PI and PVDF nanofibers as shown in Fig. 1b and c, respectively. It is found that the PI and PVDF nanofibers have average diameters of 212 nm and 317 nm from the statistical analyses of PI and PVDF nanofibers in Fig. 1d and e, respectively. These nanofibers can form non-woven mats with high porosity and tortuosity to decrease the internal charge transport resistance of battery. The porosity (P) is an important parameter for separators as it influences the electrolyte uptake and ionic conductivity [21,22]. The quantitative analysis is conducted here by using the n-butanol uptake method and calculated as [23]:

$$P(\%) = M_{BuOH}/(\rho_{BuOH} \times (M_{BuOH}/\rho_{BuOH} + M_m/\rho_P)) \times 100\%, \quad (1)$$

where M_m and M_{BuOH} represent the mass of dry membrane and absorbed n-butanol, respectively, while ρ_{BuOH} and ρ_P represent the densities of n-butanol and polymer, respectively. The electrolyte uptake (EU) can be computed as:

$$EU(\%) = (W - W_0)/W_0 \times 100\%, \quad (2)$$

where W_0 and W represent the mass of the dry membrane and wet electrolyte-absorbed membrane, respectively. Ionic conductivity (σ) can be computed as:

$$\sigma = L/(R_b \times S), \quad (3)$$

where L and R_b represent the thickness and bulk resistance of separator, respectively. S is the area of copper electrode.

Table 1 lists the experimental results on the porosity of the prototype PI/PVDF/PI separator and the PP separator (Nantong Tianfeng New Electronic Materials Co.). The thickness of the PP separator and the prototype PI/PVDF/PI separator is 40 μm and 50 μm, respectively, with measured porosity of 43.6% and 83.0% and electrolyte uptake of 62.9% and 476.0%, respectively. In other words, the new separator presented in this work has a bit larger thickness but has about twice higher porosity and more than six times higher electrolyte uptake capability – both are in favor of improving the battery performances. The tensile strength of PI/PVDF/PI separator is about 8.2 Mpa, which can meet the mechanical requirement of LIB

Table 1
The thickness, tensile strength, porosity, electrolyte uptake and ionic conductivity of PP and PI/PVDF/PI separators.

Parameters	PP	PI/PVDF/PI
Diameter (nm)	N/A	PVDF layer: 317±270 PI layer: 212±134
Thickness (μm)	40	50
Tensile strength (Mpa)	–	8.2
Porosity (%)	43.6	83.0
Electrolyte uptake (%)	62.9±6.0	476.0±6.2
Conductivity (mS cm^{-1})	0.80	3.46±0.32

production. The weight changes of PI and PVDF spincoated thin films are tested to be 0.61% and 13.45% respectively and it means that the PVDF and PI cannot swell greatly. Therefore the composite membrane will remain their structural stability.

The effects of the thermal treatments on the morphology of PI/PVDF/PI membrane are experimentally characterized. After the separators were heated at 150, 160 and 170 °C for 2 hours, the top PI layer is peeled off carefully to examine the conditions of the PVDF nanofibers as illustrated in Fig. 2a. It is found that the nanofibers were able to sustain high temperature conditions up to 150 °C without any visible changes. At 160 °C, the nanofibers start to degrade and merge together but large pores can be clearly identified after 2 hours of high temperature treatment. Under the treatment of 170 °C, PVDF nanofibers are clearly melted and merged entirely to form the pore-free layer as shown. Therefore, the shutdown function can be achieved under high temperature operations. Since high temperature process at 170 °C can result in clear shutdown behavior, we have focused our investigations next on the uptake of electrolyte under the high temperature conditions of 170 and 180 °C up to 120 minutes in Fig. 2b. Each data point is the average result of three different tests. It can be found that the average electrolyte uptake decreases from 476% initially to about 300% at the end of the high temperature treatments and most decrements occur at the first 10 minutes. Since the top and bottom PI membranes don't change their porosity in the process, they can still hold the electrolyte as the result of the final 300% electrolyte uptake. The melded PVDF nanofibers can no longer hold the electrolyte as it has lost its porosity. The inset pictures are the top view SEM images of the PVDF layer and it is observed that after just 1 minute, the nanofibers have already partially melted to have reduced porosity. Furthermore, these data suggest that at the higher temperature of 180 °C, faster melting process results in faster decrement of electrolyte uptake as shown. In either case, after about 10 minutes under high temperature treatment, the data suggest that the electrolyte uptake already reach steady-state condition or the PVDF membrane can no longer hold electrolyte uptake. In other words, a pore-free film must have been formed and it will prevent the transfer of ions and shut down battery operation. This reaction provides a unique feature for the safe operation of LIBs.

3.2. Thermal stability and thermal shrinkage

Fig. 3 shows the thermal properties of the separator. There are two great heat flow changes at about 170 °C and 500 °C. With the weight loss curve with temperature, it means that part of the separator begins to melt at about 170 °C, which is exactly the melting point of PVDF and coincides with the designed thermal shutdown temperature. The melting temperature is much higher than that of commercial PE separator, so the electrospun PI/PVDF/PI membrane has high thermal stability.

Thermal shrinkage of separator can also seriously affect the thermal stability of LIBs. For example, the commercial PE separator starts to melt when the battery temperature reaches 130 °C [24]. Separators made of PP has a higher melting temperature [25] at around 160 °C. A series of thermal treatments have been conducted at 90, 160 and 180 °C for 2 hours for the single-layer PP, PI, PVDF separators and the sandwiched PI/PVDF/PI separator and the

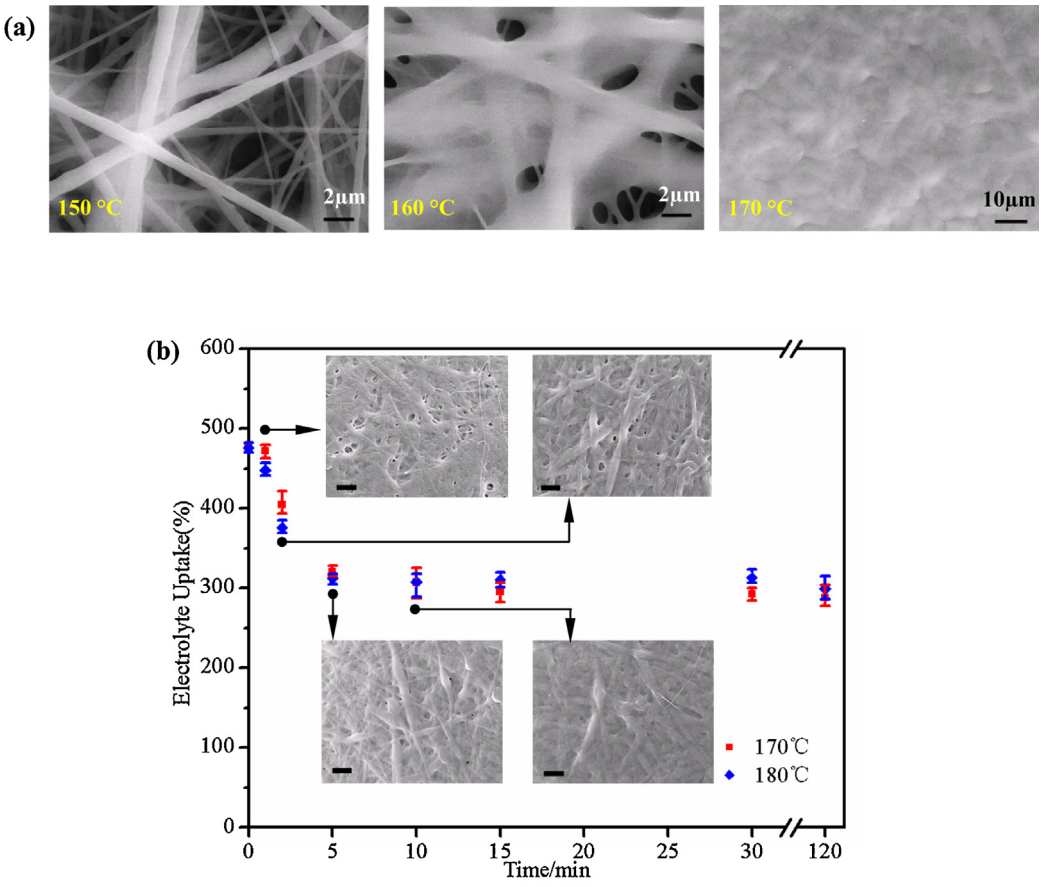

Fig. 2. (a) Top view SEM images of PVDF nanofibers layer after the thermal treatments at 150, 160 and 170 °C for 2 hours. (b) The electrolyte uptake of the electrospun PI/PVDF/PI membrane after the thermal treatment process at 170 °C and 180 °C. The inset SEM images are the PVDF layer after the thermal treatment process at 170 °C. The scale bar in the inset: 10 μm.

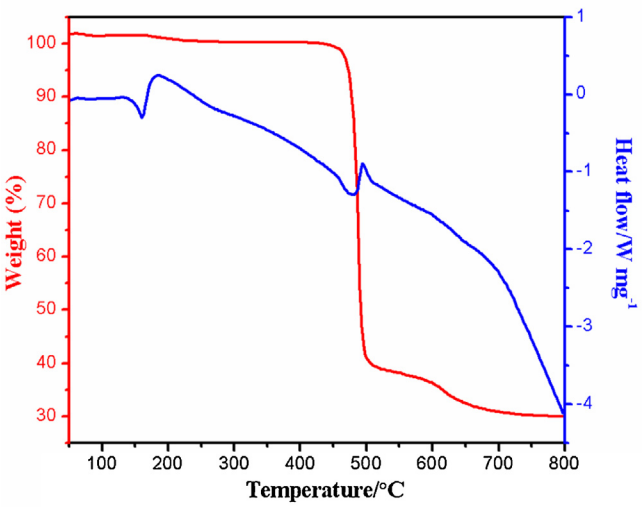

Fig. 3. TGA-DSC of electrospun PI/PVDF/PI membrane.

results are shown in Fig. 4. During the fabrication of the PP separator, a mechanical drawing process is commonly executed on the polymer sheet to generate micro-pores, and the drawing direction is defined as the machining direction as marked in the red arrow directions in Fig. 4. It is found that the PP separators shrink 2.7% and 5.4% in the machining direction after the high temperature thermal treatments at 90 °C and 160 °C, respectively. The electrospun PI/PVDF/PI separators, on the other hand, shrink with no directionality, 2.2% and 2.7% after thermal treatments at 90 °C and 160 °C, respectively. When the temperature is increased to 180 °C for 2 hours, the PP separator melts with a severely distorted shape as shown in Fig. 4(d), while the PI/PVDF/PI separator has 2.7% shrinkage similar to the result with the thermal treatment temperature at 160 °C. Fig. 4(e)-(h) are tests of single-layer electrospun PI separators and single-layer electrospun PVDF separators. Results show almost no shrinkage for these separators up to 180 °C treatments for the PI separators. On the other hand, the single-layer electrospun PVDF separators start to shrink under the 160 °C treatment and have severe distortion under the 180 °C treatment. Obviously, the commercial polyolefin separator can't maintain its original morphology when the temperature is higher than 160 °C while the electrospun PI/PVDF/PI separator can maintain its mechanical integrity at the same or higher temperature for better thermal stability.

3.3. Shutdown Electrochemical Behaviors

The shutdown function of separator can prevent thermal runaway of LIBs and is investigated further here. After the PI/PVDF/PI separator is heated at 170 °C for 2 hours, morphology changes of the separators are examined. The samples were prepared by placing a regular paper on top of the bottom PI membrane to cover about 50% of the area before the electrospinning process of the middle PVDF layer. Afterwards, the paper was removed and a second paper was placed on top of the deposited PVDF layer with a 90-degree angle to the position of the first paper before the electrospinning of the top PI layer. Afterwards, the second paper was removed to allow the exposure of the bottom PI layer, the middle PVDF layer and the top PI layer at the intersection position of the two papers as illustrated in the SEM image of Fig. 5a after the 170 °C for 2 hours thermal treatment process. It is observed as before that the PI nanofibers maintain their original morphology while PVDF nanofibers have melted and formed a continuous membrane without pores as depicted in the close-view SEM image in Fig. 5b. The close-view SEM photo in Fig. 5c further confirms that there are no observable penetrating holes on the PVDF membrane as PVDF nanofibers have melted to form a continuous film. This effect should be able to effectively cut off the ion transfer channels between the two electrodes and shutdown the operation of the battery to prevent thermal runaway.

Electrochemical tests on CR2016 coin cells with PI/PVDF/PI separator before and after the thermal treatments at 160 °C and 170 °C for 2 hours have been conducted. The charge and discharge behaviors of the prototype coin cells are similar with and without the thermal treatment at 160 °C as shown in Fig. 5d and e with measured capacities around 107 mAh g^{-1}. On the other hand, for the cells after the 170 °C thermal treatment process, the cell potential during the charging cycle increases sharply from 3.00 to 4.66 V at the initial galvanostatic charging stage and decreases instantly to 4.3 V, while the current decreases to zero in a very short time as shown in Fig. 5f. During the galvanostatic discharging stage, the cell potential decreases instantly to 3.66 V. The measured discharge capacities are only about 7% of those of the normal cells

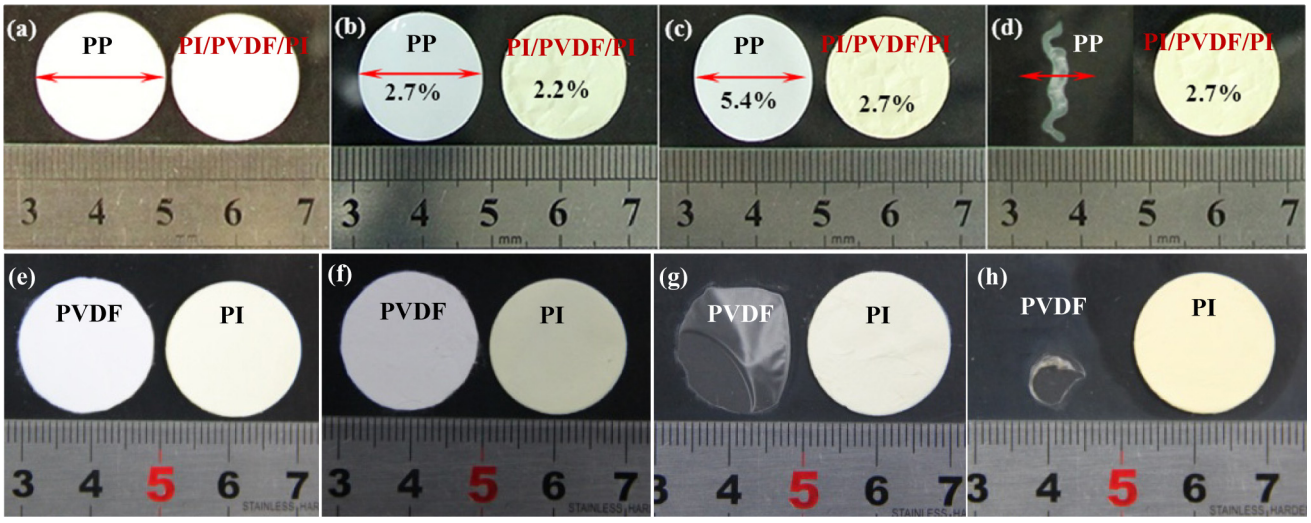

Fig. 4. (a - d) Optical photos of PP and PI/PVDF/PI separators before and after the thermal treatments for 2 hours; (a) before the thermal treatment; (b) 90; (c) 160; and (d) 180 °C. The data inserted in (b - d) represent the shrinkage percentages and the red arrows are machining directions for the PP separator. (e - h) Optical photos of the single-layer PVDF nanofibers separators and PI nanofibers separators before and after the thermal treatments for 2 hours; (e) before the thermal treatment; (f) 90; (g) 160; and (h) 180 °C for the thermal treatment temperature.

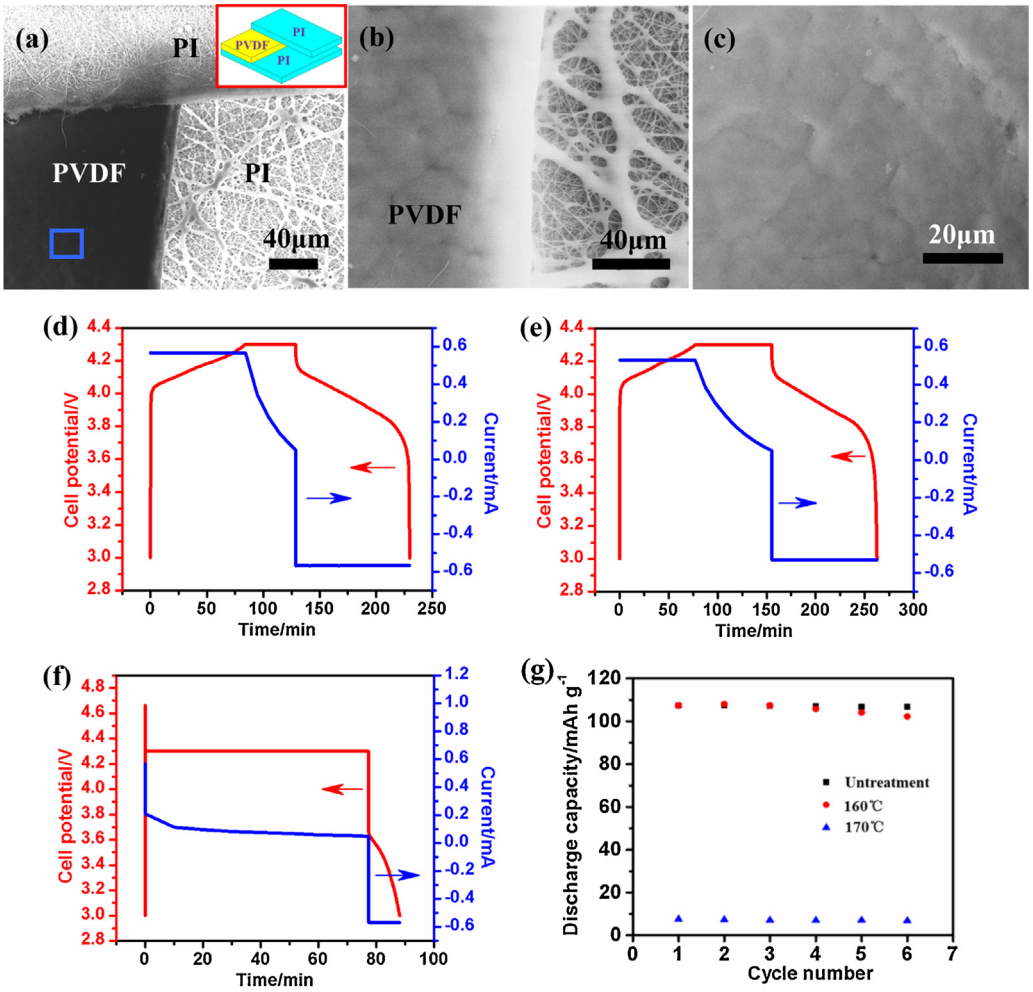

Fig. 5. (a - c) SEM images of PI/PVDF/PI separators after the thermal treatment at 170 °C for 2 hours. (a) PI nanofibers have maintained their original shapes while PVDF nanofibers have formed a continuous film; (b) close-up image showing the intersection areas of PVDF film and PI nanofibers; and (c) close-up SEM photo of the PVDF film without observable penetrating pores. (d - f) Charging and discharging results with voltage/current versus time for the CR2016-type coin cells using the PI/PVDF/PI separator. (d) Before any thermal treatment; (e) after the thermal treatment at 160 °C for 2 hours; (f) after the thermal treatment at 170 °C for 2 hours. (g) Battery discharging cycle performances.

as seen in Fig. 5 g. This result implies that the charge transfer must have been severely blocked as the result of the melted PVDF nanofibers resulting in pore-free membrane. This is further evidenced in Fig. 5f that during the charging stage, the magnitude of the measured current is close to zero. Previous works have shown that when the PVDF membrane is at the swollen gel phase, it offers a tiny ionic conductivity [21,26] which could be the potential leakage currents our measurement results. Nevertheless, the shutdown functions of LIBs have been validated as shown.

3.4. Impedance and Cycling Tests

The ionic conductivity of PI/PVDF/PI separator has been measured as 3.46 mS cm^{-1}, while the PP separator has a much lower number at 0.80 mS cm^{-1} at room temperature. In other words, the composite separator does provide better ionic conductivity mainly due to its high porosity as compared with the PP separator for superior battery performances. Fig. 6a further records the AC impedance spectroscopies of the PI/PVDF/PI separators and PP separators at room temperature. As illustrated in the lower right insert, the impedance spectroscopies were tested by the sandwiched copper/separator/copper structure and the EIS method. Compared with the PP separators, the curves of the PI/PVDF/PI separators have shifted leftwards and their impedance values are about one-third of those of PP separators due to high porosity. The cell cycle test is also characterized with LIBs using the prototype PI/PVDF/PI separator and the standard PP separator (TFA, 40 μm in thickness) at 0.5C rates. As depicted in Fig. 6b, the initial discharge capacity of the cell with the PI/PVDF/PI and PP separators are 114.8 mAh g^{-1} and 111.5 mAh g^{-1}, respectively. The discharge capacity retention ratio of the battery cells using the PI/PVDF/PI separator is 97.1% of the initial discharge capacity after 100 cycles and the battery cells using the commercial PP separator is only 96.3%. The better performance can be attributed to the higher porosity and electrolyte uptake of the PV/PVDF/PI separator [27]. The rate capability tests have also been measured by charging the cells at the 0.2C-rate to 4.2 V, and discharging them at the 0.1, 0.2, 0.5, 1 and 2C-rate of 5 cycles each to 3.6 V in sequence as shown in Fig. 6c. It is found that a high discharge capacity of 114.5 mAh g^{-1} at 0.1C has been achieved. When the discharge rate is increased to the 2C-rate, the discharge capacity retention ratio is 95.1%, which is similar to the cells using the PP separator. Furthermore, in all tests, the cells with the PI/VPDF/PI separators have shown higher discharge capacity than those of cells using the PP separators. It is believed that the high porosity and interconnected pores for the PI/PVDF/PI separator result in high electrolyte uptake, high ionic conductivity and fast transfer paths for lithium ions for reduced internal impedance of battery and high discharge capacity [28].

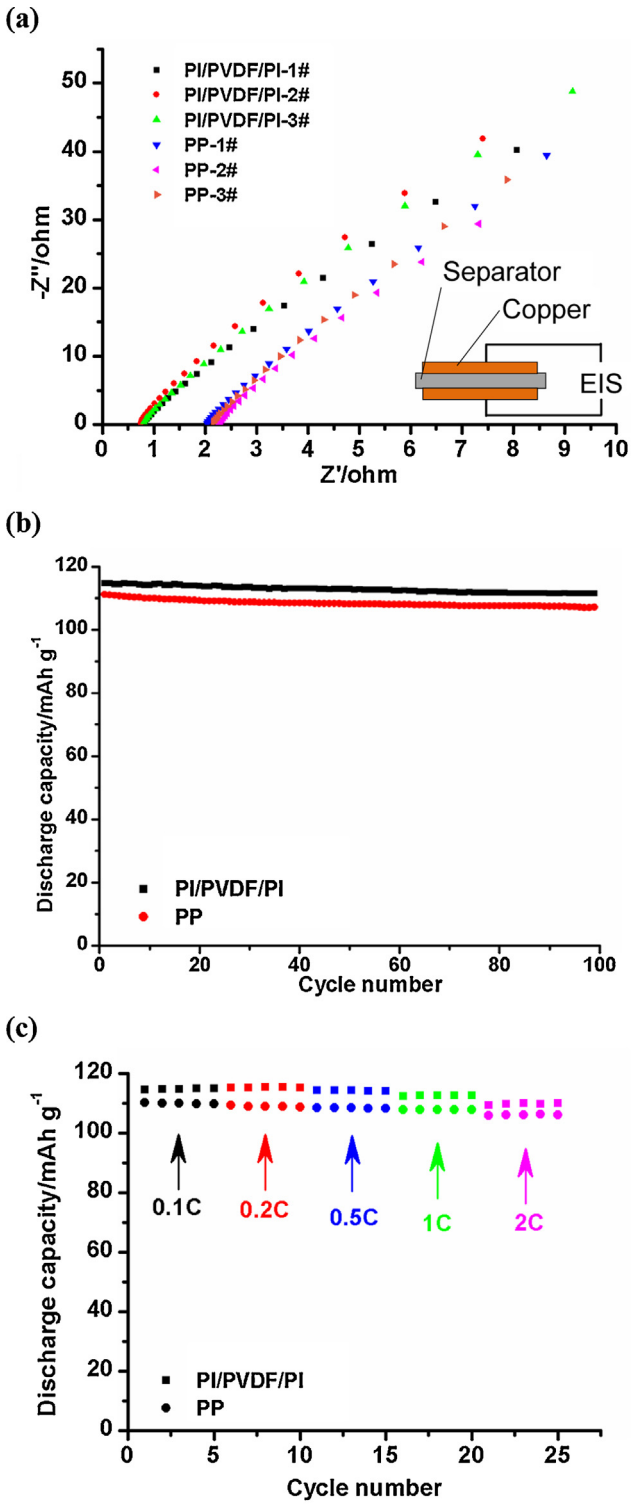

Fig. 6. (a) AC impedance spectroscopies of the PP separators and PI/PVDF/PI membranes at room temperature. (b) Battery cycle performance using the PI/PVDF/PI and PP separators under 100 cycles of the 0.5C charge/discharge rate. (c) Rate capacity tests for the cells using the PI/PVDF/PI and PP separators.

4. Conclusions

The electrospun sandwiched PI/PVDF/PI separators have been demonstrated and characterized in LIBs to achieve improved performances as compared with batteries using the PP separators, including thermal stability, impedance, cycling life, and charge/discharge retention rates. The new separators have high ionic conductivity of 3.46 mS cm^{-1} at room temperature, low specific capacity decay rate of 2.9% after 100 cycles under 0.5C-rate discharges, and excellent retention rate at 95.1% of the initial discharge capacity under the 2C-rate discharge tests. Furthermore, the shutdown function under high temperature operation of the PI/PVDF/PI separator could be vital to prevent the thermal runaway issues of LIBs.

Acknowledgements

This work was supported by the National Natural Science Foundation of China (No.51205334), National High Technology Research and Development Program (No.2012AA110404) and Science and Technology Program of Shenzhen City (No. JCYJ20120615161609592).

References

[1] Y.-G. Guo, J.-S. Hu, L.-J. Wan, Nanostructured Materials for Electrochemical Energy Conversion and Storage Devices, Advanced Materials 20 (2008) 2878–2887.
[2] H. Yoneda, Y. Nishimura, Y. Doi, M. Fukuda, M. Kohno, Development of microporous PE films to improve lithium ion batteries, Polymer Journal 42 (2010) 425–437.
[3] M.-L. Lee, Y.-H. Li, J.-W. Yeh, H.C. Shih, Improvement in safety and cycle life of lithium-ion batteries by employing quercetin as an electrolyte additive, Journal of Power Sources 214 (2012) 251–257.
[4] H.F. Xiang, B. Yin, H. Wang, H.W. Lin, X.W. Ge, S. Xie, C.H. Chen, Improving electrochemical properties of room temperature ionic liquid (RTIL) based electrolyte for Li-ion batteries, Electrochimica Acta 55 (2010) 5204–5209.
[5] F.-M. Wang, S.-C. Lo, C.-S. Cheng, J.-H. Chen, B.-J. Hwang, H.-C. Wu, Self-polymerized membrane derivative of branched additive for internal short protection of high safety lithium ion battery, Journal of Membrane Science 368 (2011) 165–170.
[6] M. Kim, J.H. Park, Inorganic thin layer coated porous separator with high thermal stability for safety reinforced Li-ion battery, Journal of Power Sources 212 (2012) 22–27.
[7] T.-H. Cho, M. Tanaka, H. Ohnishi, Y. Kondo, M. Yoshikazu, T. Nakamura, T. Sakai, Composite nonwoven separator for lithium-ion battery: Development and characterization, Journal of Power Sources 195 (2010) 4272–4277.
[8] C. Shi, P. Zhang, L. Chen, P. Yang, J. Zhao, Effect of a thin ceramic-coating layer on thermal and electrochemical properties of polyethylene separator for lithium-ion batteries, Journal of Power Sources 270 (2014) 547–553.
[9] D. Wu, S. Huang, Z. Xu, Z. Xiao, C. Shi, J. Zhao, R. Zhu, D. Sun, L. Lin, Polyethylene terephthalate/poly (vinylidene fluoride) composite separator for Li-ion battery, Journal of Physics D: Applied Physics 48 (2015) 285305.
[10] Y. Liang, L. Ji, B. Guo, Z. Lin, Y. Yao, Y. Li, M. Alcoutlabi, Y. Qiu, X. Zhang, Preparation and electrochemical characterization of ionic-conducting lithium lanthanum titanate oxide/polyacrylonitrile submicron composite fiber-based lithium-ion battery separators, Journal of Power Sources 196 (2011) 436–441.
[11] W. Qi, C. Lu, P. Chen, L. Han, Q. Yu, R. Xu, Electrochemical performances and thermal properties of electrospun Poly(phthalazinone ether sulfone ketone) membrane for lithium-ion battery, Materials Letters 66 (2012) 239–241.
[12] N. Wu, Q. Cao, X. Wang, S. Li, X. Li, H. Deng, In situ ceramic fillers of electrospun thermoplastic polyurethane/poly(vinylidene fluoride) based gel polymer electrolytes for Li-ion batteries, Journal of Power Sources 196 (2011) 9751–9756.
[13] P. Carol, P. Ramakrishnan, B. John, G. Cheruvally, Preparation and characterization of electrospun poly(acrylonitrile) fibrous membrane based gel polymer electrolytes for lithium-ion batteries, Journal of Power Sources 196 (2011) 10156–10162.
[14] K. Hwang, B. Kwon, H. Byun, Preparation of PVdF nanofiber membranes by electrospinning and their use as secondary battery separators, Journal of Membrane Science 378 (2011) 111–116.
[15] J.-K. Kim, L. Niedzicki, J. Scheers, C.-R. Shin, D.-H. Lim, W. Wieczorek, P. Johansson, J.-H. Ahn, A. Matic, P. Jacobsson, Characterization of N-butyl-N-methyl-pyrrolidinium bis(trifluoromethanesulfonyl) imide-based polymer electrolytes for high safety lithium batteries, Journal of Power Sources 224 (2013) 93–98.
[16] J. Hao, G. Lei, Z. Li, L. Wu, Q. Xiao, L. Wang, A novel polyethylene terephthalate nonwoven separator based on electrospinning technique for lithium ion battery, Journal of Membrane Science 428 (2013) 11–16.
[17] Y.-E. Miao, G.-N. Zhu, H. Hou, Y.-Y. Xia, T. Liu, Electrospun polyimide nanofiber-based nonwoven separators for lithium-ion batteries, Journal of Power Sources 226 (2013) 82–86.
[18] N. Angulakshmi, A.M. Stephan, Electrospun Trilayer Polymeric Membranes as Separator for Lithium–ion Batteries, Electrochimica Acta 127 (2014) 167–172.

[19] J. Lee, C.-L. Lee, K. Park, I.-D. Kim, Synthesis of an Al_2O_3-coated polyimide nanofiber mat and its electrochemical characteristics as a separator for lithium ion batteries, Journal of Power Sources 248 (2014) 1211–1217.
[20] K.S. Jeon, R. Nirmala, R. Navamathavan, K.J. Kim, S.H. Chae, T.W. Kim, H.Y. Kim, S.J. Park, The study of efficiency of Al_2O_3 drop coated electrospun meta-aramid nanofibers as separating membrane in lithium-ion secondary batteries, Materials Letters 132 (2014) 384–388.
[21] S.W. Choi, S.M. Jo, W.S. Lee, Y.-R. Kim, An electrospun poly (vinylidene fluoride) nanofibrous membrane and its battery applications, Advanced Materials 15 (2003) 2027–2032.
[22] J.-K. Kim, G. Cheruvally, X. Li, J.-H. Ahn, K.-W. Kim, H.-J. Ahn, Preparation and electrochemical characterization of electrospun, microporous membrane-based composite polymer electrolytes for lithium batteries, Journal of Power Sources 178 (2008) 815–820.
[23] J.R. Kim, S.W. Choi, S.M. Jo, W.S. Lee, B.C. Kim, Characterization and Properties of P(VdF-HFP)-Based Fibrous Polymer Electrolyte Membrane Prepared by Electrospinning, Journal of The Electrochemical Society 152 (2005) A295.
[24] L. Lu, X. Han, J. Li, J. Hua, M. Ouyang, A review on the key issues for lithium-ion battery management in electric vehicles, Journal of Power Sources 226 (2013) 272–288.
[25] W. Jiang, Z. Liu, Q. Kong, J. Yao, C. Zhang, P. Han, G. Cui, A high temperature operating nanofibrous polyimide separator in Li-ion battery, Solid State Ionics 232 (2013) 44–48.
[26] J. Saunier, F. Alloin, J.Y. Sanchez, G. Caillon, Thin and flexible lithium-ion batteries: investigation of polymer electrolytes, Journal of Power Sources 119-121 (2003) 454–459.
[27] Y. Liang, Z. Lin, Y. Qiu, X. Zhang, Fabrication and characterization of LATP/PAN composite fiber-based lithium-ion battery separators, Electrochimica Acta 56 (2011) 6474–6480.
[28] X. Li, G. Cheruvally, J.-K. Kim, J.-W. Choi, J.-H. Ahn, K.-W. Kim, H.-J. Ahn, Polymer electrolytes based on an electrospun poly(vinylidene fluoride-co-hexafluoropropylene) membrane for lithium batteries, Journal of Power Sources 167 (2007) 491–498.